Fouling control in reverse osmosis membranes through modification with conductive carbon nanostructures

Farah Ejaz Ahmed[1], Raed Hashaikeh[1*], Nidal Hilal[1,2]

[1] Engineering Division, NYUAD Water Research Center, New York University Abu Dhabi, Abu Dhabi, United Arab Emirates

[2] Centre for Water Advanced Technologies and Environmental Research (CWATER), College of Engineering, Swansea University, Fabian Way, Swansea SA1 8EN, UK

*raed.hashaikeh@nyu.edu

Abstract

A conductive form of networked cellulose, prepared by incorporating carbon nanotubes, has been used in polyvinyl alcohol (PVA) membranes for reverse osmosis. The use of networked cellulose and carbon nanostructures (CNS) not only helps control the thermal, mechanical and electrical properties of the membrane, but also enhances RO performance and allows the membrane surface to be cleaned electrolytically. High surface area multi-walled CNTs become trapped in the structure of networked cellulose. The modified material has greater tensile strength and elastic modulus, indicating an improvement in the mechanical properties of the membrane. Membranes with CNS demonstrate enhanced electrocatalytic activity when tested for hydrogen evolution in an acidic medium. The membranes are successfully applied to reverse osmosis using a feed of 25000 ppm NaCl, where the membranes with 7 wt. % CNS exhibited a 93% increase in flux compared to PVA-NC with no CNS, due to the nanotubes disrupting the compression of polymer chains under pressure. The membrane surface was recovered after fouling via electrolytic cleaning where the membrane was used as the cathode and a potential of -5V was applied for 20 minutes. All membranes retained a high salt rejection above 99.8%.

Keywords: reverse osmosis, carbon nanotubes, cellulose, electrically conductive membrane

1. Introduction

Population growth and limited fresh water resources have driven an increase in desalination installation capacity in the last several decades. The UN World Water Development Report states that 3.7 billion people are affected by water scarcity at present [1]. Although thermal processes have been traditionally applied, lower costs of and the ability to tailor membrane materials has caused the market share of membrane-based desalination to rapidly rise in the last several decades. Reverse osmosis (RO), in particular, is the fastest growing desalination technology in the world [2, 3]. RO relies on a dense semipermeable membrane separating the salty feed and clean permeate, wherein separation takes place by solution diffusion through the membrane material. Although there have been significant advances in membrane materials for RO, the process is limited by the occurrence of fouling which leads to deterioration of membrane performance and shortens its lifetime. As a result, functional materials with the ability to prevent fouling while retaining superior membrane performance are desirable, with the goal of minimizing cleaning frequency and energy costs associated with cleaning and membrane replacement. In the last few years, research has rapidly grown in the area of electrically conductive fillers, such as carbon nanotubes (CNTs), in polymeric membranes [4, 5]. These membranes have been applied to electrically enhanced fouling control through oxidation of foulants, physical sweeping via bubble generation, inherent antimicrobial properties of the filler as well as electrophoretic transport of foulants [6-8]. For reverse osmosis, the challenge is to modify existing membranes to enhance their electrocatalytic activity while retaining a hydrophilic, non-porous membrane with high selectivity and water permeation. A few studies have focused on developing electrically conductive membranes for ultrafiltration [9], nanofiltration [10],

reverse osmosis [11] and more recently, forward osmosis [12].

Despite its swelling capacity, polyvinyl alcohol (PVA) has widely been investigated as a promising material in membrane-based separation technologies due to excellent film forming ability and hydrophilicity [13]. Recently, Anis *et al.* used networked cellulose (NC) to control the swelling of PVA membranes for RO. Apart from biodegradability and biocompatibility, the world's most abundant natural raw material also offers high chemical stability. NC is a form of cellulose obtained through controlled dissolution in sulphuric acid followed by regeneration [14]. In a previous study, an electrically conductive form of NC prepared using CNTs, known as NC-CNS was shown to be effective as a cathode for hydrogen evolution reaction (HER) [10], which renders it an attractive material for electrolytic self-cleaning membranes.

This study builds on previous work to develop electrically conductive RO membranes based on PVA, incorporated with NC-CNS. The incorporation of NC-CNS in self-supporting PVA membranes provides control over their mechanical, thermal, electrical properties and RO performance such that they can potentially be used for *in situ* electrolytic cleaning. The performance of this novel membrane material is studied with respect to electrocatalytic activity and reverse osmosis, in an attempt to identify its potential as a self-cleaning reverse osmosis membrane

2. Materials and methods

2.1 Materials

Polyvinyl alcohol (PVA, Mw = 145,000), ethanol and sulfuric acid were purchased from Aldrich. Microcrystalline cellulose (MCC), Avicel PH 101, (Mw: 160 kDa–560 kDa), was

purchased from FMC Biopolymer (USA). CNS (with an average length of 300 μm) was developed by Applied NanoStructured Solutions, LLC through a continuous chemical vapor deposition process [4,14]. Yeast (Baker's yeast, DCL, France) and humic acid (Aldrich) were used as model foulants. All materials were used as received.

Preparation of networked cellulose (NC) has been described elsewhere [10, 14]. Conductive NC was prepared by adding 2 g CNS for every 10 g MCC 10 minutes before regeneration with chilled ethanol such that the ratio of NC:CNS by weight is 5:1. This ratio was chosen on the basis of lowering CNS in large amounts during regeneration of networked cellulose.

2.2 Membrane fabrication

A 5 wt% PVA solution was first prepared by stirring PVA powder in DI water at 150 °C until a clear solution was obtained. Membranes were prepared with 0, 3, 5 and 7 wt% CNS, using a solution casting procedure described by Anis *et al.* [13]. NC or NC-CNS suspension was gently stirred in varying amounts with PVA solution at varying content and cast in an aluminum dish and subsequently dried for 3 days at room temperature. Table 1 shows the PVA, NC, CNS content in the prepared membrane samples.

Table 1. PVA, NC, CNS content in prepared membrane samples

Sample	PVA	NC	CNS
PVA-NC-0CNS	80 wt%	20 wt%	0 wt%
PVA-NC-3CNS	81 wt%	16 wt%	3 wt%
PVA-NC-5CNS	67 wt%	27 wt%	5 wt%
PVA-NC-7CNS	58 wt%	35 wt%	7 wt%

2.2. Characterization

2.2.1. Morphology

Morphology of the PVA-NC membranes with and without CNS was examined using field-enhanced scanning electron microscopy (FEI Quanta 450 FEG, Netherlands) under high vacuum. The samples with 0 and 3 wt. % CNS were first gold coated using the 108 Auto Sputter Coater (Ted Pella, USA).

2.2.2. Structure (TEM)

In order to examine the structure of the PVA-NC membrane with and without CNS, the PVA-NC and PVA-NC-CNS suspensions were observed under a transmission electron microscope (FEI TEM Talos F200X). To prepare TEM samples, a small amount of 5 wt.% PVA solution was mixed with a few drops of either NC or NC-CNS, diluted with water and bath sonicated for 10 minutes. A droplet of each resulting suspension was then dried on a carbon coated copper grid.

2.2.3 Wettability

To examine, the wettability of the membrane surface to water, contact angle measurements were taken on an EasyDrop Standard drop shape analysis (KRUSS, Germany) using deionized water. Digital images of 2 μL water droplets on the membrane surface were captured and used to measure the contact angle using the sessile drop technique. An average of three measurement values was then recorded as the water contact angle.

Three measurements were taken for each sample and the average of these values was recorded.

2.2.4. Tensile testing

Tensile testing was carried out to examine the mechanical properties of the PVA-NC-CNS membranes on the Instron 5966 Dual Column Tabletop Testing System (Italy). Standard dog-bone specimens were stretched in tension at a strain rate of 1 mm/min until failure. The stress response was measured and used to generate stress-strain curves, from which key properties such as elastic modulus, tensile strength and % elongation at failure were obtained. Young's modulus is calculated by taking the ratio of tensile stress to strain in the elastic region, and is a measure of the stiffness of the material.

2.2.4. Thermal stability

Thermal analysis of PVA-NC and PVA-NC-CNS membranes was carried out using thermogravimetric analysis (TGA) and differential scanning calorimetry (DSC) using TA Instruments SDT-Q600 TGA/DSC (Delaware, USA). A sample of known mass was placed in an alumina crucible next to an identical reference pan. The sample and reference pans are then heated from room temperature to 800 °C at a rate of 10 °C/min under a nitrogen atmosphere.

2.2.4. Electrochemical properties

Linear polarization (LP) and impedance measurements were performed on Autolab302N potentiostat/galvanostat using a three-electrode system, where PVA-NC-CNS acted as the working electrode, Pt as the counter electrode and Ag/AgCl (3.5 M KCl solution) as the reference electrode. In the case of LP, Measured potentials are converted to RHE by adding a value of 0.205 + 0.059pH) V. The working electrodes have an area of 1 cm^2. For electrochemical impedance spectroscopy (EIS), an alternating voltage of 100 mV was applied at 50 frequencies over a range of 10^{-2} to 10^5 Hz in a logarithmic distribution, and

the current developed was used to calculate the impedance. The potentiostat has a current accuracy of ± 0.2%. Before running LP scans, all the electrodes were run for ten cyclic voltammetry curves in the appropriate potential range for HER to stabilize the electrodes.

2.3. Reverse osmosis

For RO testing, membranes with a diameter of 8.5 cm were wet with water. Pure water was passed through the PVA-NC-CNS membranes at a pressure of 22 bars for 30 minutes. RO tests were carried out for each membrane using an aqueous solution of 25000 ppm NaCl as feed at a pressure of 24 bars for a duration of 60 minutes, using the setup shown in **Figure 1**.

Figure 1: Lab-scale RO unit used for RO experiments

Two performance parameters, namely flux and salt rejection rate, were determined. Salt rejection (SR) was calculated using the following formula:

$$\%SR = \frac{C_{feed} - C_{permeate}}{C_{permeate}}$$

Where C_{feed} and $C_{permeate}$ are the feed and permeate NaCl concentrations (ppm), respectively. Permeate concentration is obtained by converting permeate conductivity,

measured on accumet® XL 50 dual channel pH/Ion/conductivity meter to total dissolved solids (TDS).

2.4 Membrane fouling and electrolysis

Based on RO performance, PVA-NC-7CNS was selected for fouling experiments. A model foulant solution was prepared by stirring 500 mg/L humic acid powder and 500 mg/L yeast in DI water under continuous stirring for 24 hours. The membranes were dipped in the foulant solution for 48 hours to induce membrane fouling. The fouled membrane was then removed from solution and dried at room temperature. In the electrolysis experiment, the fouled membrane was used as the working electrode, a platinum rod was used as the counter electrode while an Ag/AgCl reference electrode was employed. An aqueous solution of 25000 ppm NaCl was used as electrolyte. Electrolysis was carried out using Autolab potentiostat, where a voltage of -5V was applied for 20 minutes. The membrane was removed after electrolysis and dried at room temperature. Optical images of the membrane before and after electrolysis were obtained on a Leica M205C stereomicroscope (Leica Microsystems GmbH, Germany).

3. Results and discussion

3.1. Morphology and structure

Figure 2 shows SEM images of the PVA-NC-CNS membranes with increasing NC-CNS content, with the insets showing water droplets on the membrane surface. The surface of the PVA-NC-0CNS and PVA-NC-3CNS membranes appears to have an uneven surface due to the presence of cellulose, although CNTs are not yet visible. With increasing NC-CNS (**Figure 2c and 2d**), however, the morphology of the membrane is drastically affected

and bundles of CNTs can be observed on the membrane surface, caught in the networked cellulose.

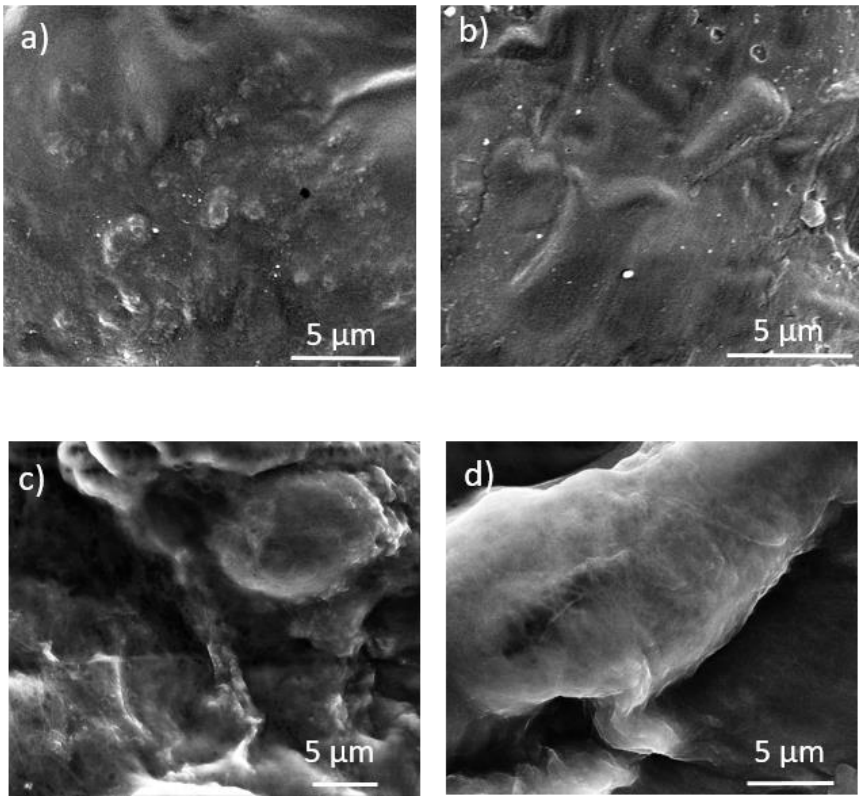

Figure 2: SEM images of the surface of a) PVA-NC-0CNS, b) PVA-NC-3CNS, c) PVA-NC-5CNS, d) PVA-NC-7CNS membranes. The inlets show water droplets on each of the membrane surfaces.

Figure 3 shows TEM images of PVA-NC a) without CNS and b) with CNS. The network structure of cellulose resulting from random bundling of chains during regeneration is characteristic of NC [13, 14]. **Figure 3b** confirms a homogeneous distribution of high aspect ratio carbon nanotubes entrapped in NC. The high aspect ratio of the tubes indicates a large surface area. A high surface area will play a role in the electrocatalytic behavior of the composite membranes, which could be beneficial for self-cleaning via electrolysis. It is important to note that the CNS:NC ratio used in the pre-prepared samples was kept at 1:5 for all samples. This ratio has been identified before through unreported data to

minimize aggregation issues during regeneration of networked cellulose. A more interconnected network of CNS across NC is likely to be achieved by increasing this ratio during the preparation of NC-CNS suspension.

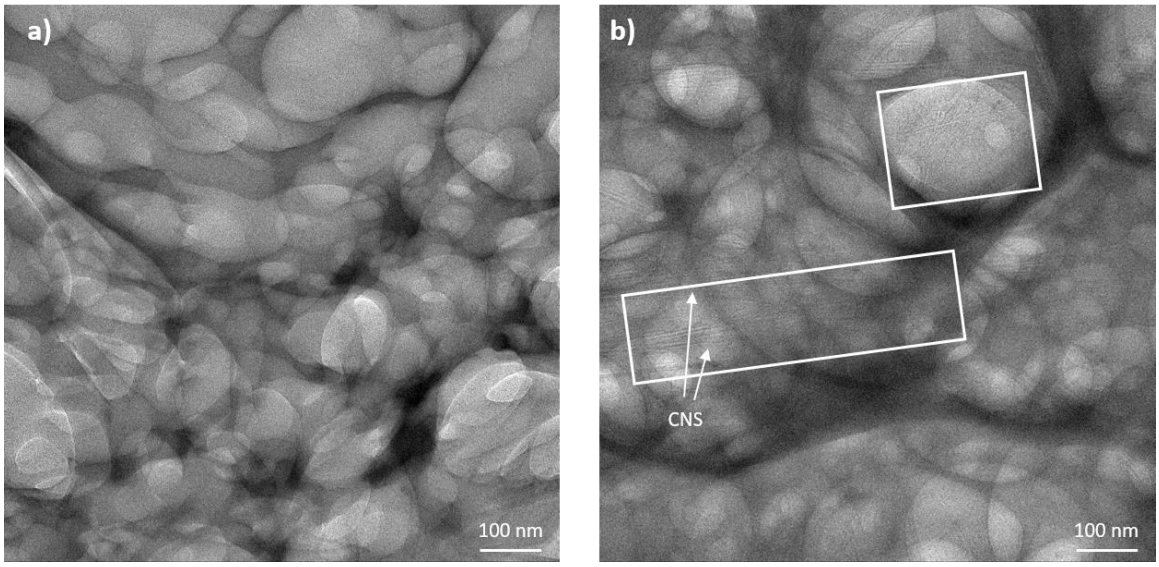

Figure 3: TEM images of PVA-NC a) without CNS and b) with CNS

3.2 Wettability

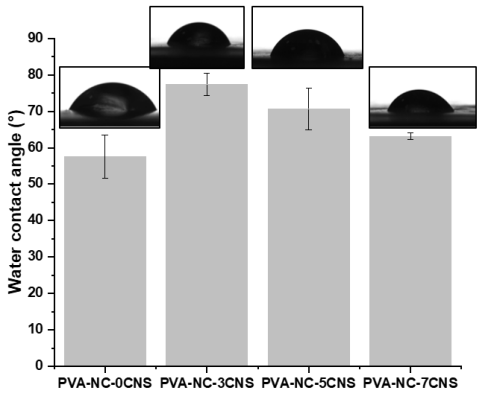

Figure 4: Water contact angle of PVA-NC-CNS membranes with varying NC-CNS content

Contact angle tests were carried out to investigate the wettability of the PVA-NC-CNS membranes with water. The values are shown in **Figure 4**, while images of the water

droplet on the membrane surface are shown in the inlets of **Figure 2**. Although the contact angle increases from 58 to 77° from without CNS to 3 wt. % CNS, it decreases slightly with increasing CNS content despite the hydrophobicity of CNS [10], due to simultaneously increasing NC content. The amorphous open structure of NC enables it to readily uptake water and thus contributes to the hydrophilicity of the material. All the composite membranes are hydrophilic, with a water contact angle of less than 80°. Hydrophilicity is a desirable property for reverse osmosis membranes as it translates into improved water flux as well as better resistance to fouling by hydrophobic foulants that are present in seawater in the form of Natural Organic Matter (NOM) [15, 16].

3. Tensile testing

The mechanical behavior of the PVA-NC-CNS membranes with different amounts of NC-CNS was investigated. Stress-strain curves for the membranes are shown in **Figure 5**. Initially, the incorporation of filler leads to an increase in tensile strength, elastic modulus, as well as ductility as can be seen in **Figure 6**. As the amount of filler is further increased however, the tensile strength and modulus continue to increase but the ductility of the material, indicated by % elongation, starts to decrease. CNS are composed of randomly oriented multi-walled carbon nanotubes. When introduced to the membrane, the CNS fibers are able to align themselves with stress direction, resulting in greater elongation at break. However, as the NC content is also simultaneously increasing, this leads to an increase in stiffness and sharp drop in elongation from 199% in PVA-NC-3CNS to 27.2% and 7.7% PVA-NC-5CNS and PVA-NC-7CNS membranes, respectively (**Figure 6**). The contribution from NC to the stiffness and ductility are greater than that from the CNTs. Tensile strength increases from 16.8 to 41.8 MPa between PVA-NC-0CNS to PVA-NC-

7CNS.

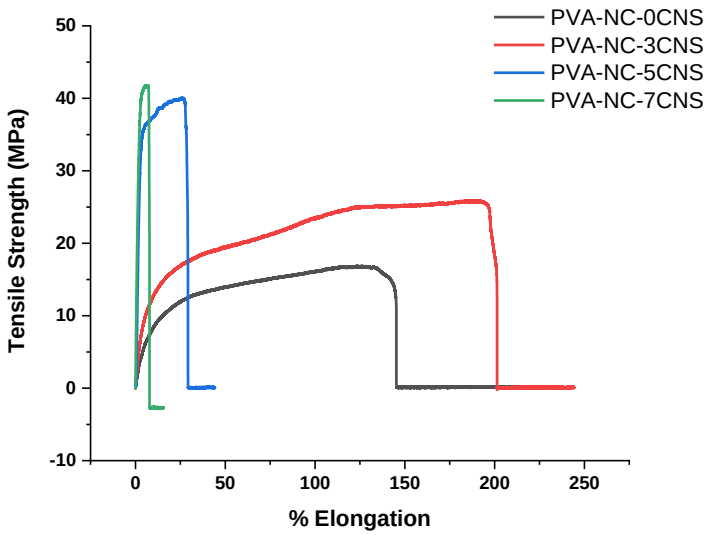

Figure 5: Stress-strain for PVA-NC-CNS membranes with varying NC-CNS content

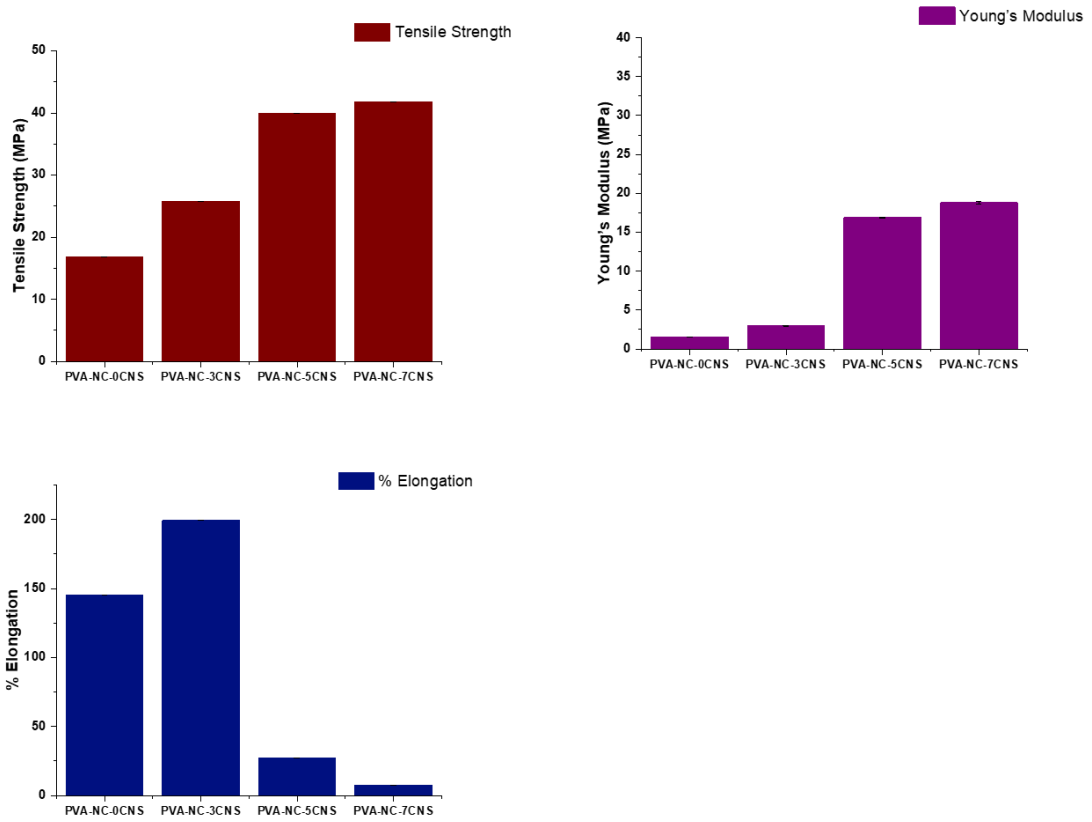

Figure 6: Mechanical properties of the membranes with varying NC-CNS content: a) tensile strength, b) Young's modulus, c) % elongation

3.4. Thermal stability

Thermal properties of the membranes with increasing amounts of CNS were studied with TGA and DSC. Typically, a baseline shift in the endothermic direction at 75 °C should be observed indicating the glass transition temperature of PVA. However, in the DSC curves obtained (**Figure 7a**), it was not possible to resolve the glass transition of PVA from the broad boiling peak due to evaporation of bound water in the samples. PVA is known to be sensitive to moisture and thus there is a significant endothermic peak from the evaporation of moisture. Another possible explanation is that the sample was only heated once and this may not be sufficient to observe the glass transition [17]. The melting point of the

membranes as obtained from DSC data is between 223 °C and 225 °C, in agreement with values from literature [17]. It is interesting to observe that the melting peak becomes narrower when the amount of CNS in the sample is increased from 3 to 5 wt. %. A narrower melting peak indicates an increase in crystallinity and could be due to the presence of carbon nanotubes, which have been shown to serve as nucleation sites for crystallization of PVA [17, 18]. TGA thermograms shown in **Figure 7b** indicate that the membranes are stable until about 205 °C, after which both PVA and NC begin to decompose. Weight loss occurs in three distinct stages. The first is attributed to the vaporization of water, while the second and third that occur after 210 °C correspond to the thermal decomposition of the PVA and NC. Carbon nanotubes retain their stability in a nitrogen atmosphere in the range of temperatures studied. The membranes are thermally stable up to 210 °C. The CNS content can also be confirmed by the TGA thermograms as the weight % of the sample after complete polymer degradation has occurred (at ~470 °C) increases with wt. % CNS.

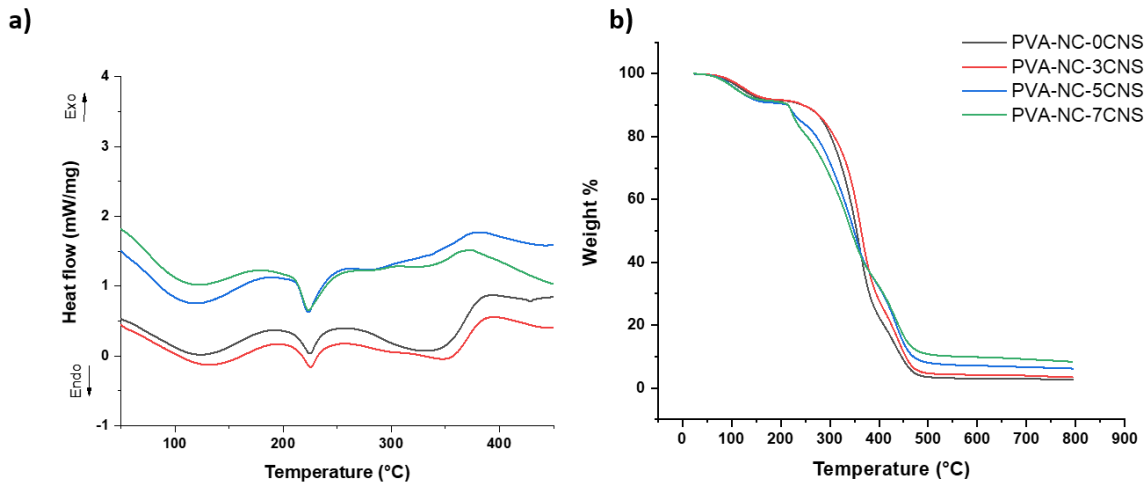

Figure 7: DSC and TG curves for PVA-NC membranes with CNS

3.5 Electrochemical measurements

Electrocatalytic activity of the PVA-NC-CNS membranes was evaluated in acidic media

using 0.5 M H_2SO_4 through linear polarization, from which Tafel curves were generated. **Figure 8** shows the polarization and Tafel curves of PVA-NC-CNS membranes for hydrogen evolution reaction (HER) in 0.5 M H_2SO_4 at a scan rate of 50 mV/s. When tested for HER in acidic media, the coefficients of charge transfer, indicated by the Tafel slope, are shown in Table 2. The charge transfer coefficient and current density increases from PVA-NC-3CNS to PVA-NC-5CNS with as CNS content is increased from 3 wt% to 5 wt%. However, when at 7 wt.% CNS content, the charge transfer coefficient and the current density decreased due to simultaneous increase in non-conducting NC content. The NC which traps CNS inside it possibly prevents the formation of a continuously connected network of CNS with PVA.

Table 2: Tafel slopes for CNS-modified PVA-NC membranes for HER in acidic medium

Membrane	Tafel slope (V/dec)
PVA-NC-3CNS	0.348
PVA-NC-5CNS	1.14
PVA-NC-7CNS	0.765

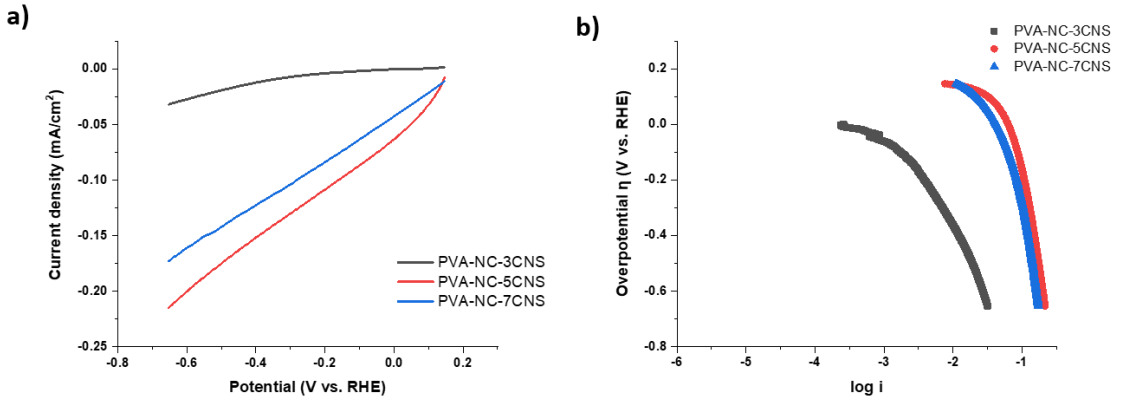

Figure 8: Linear polarization curves (a) and Tafel plots (b) of different electrodes for hydrogen evolution generation in

0.5 M H_2SO_4

3.6 Reverse osmosis performance

The PVA-NC and PVA-NC-CNS membranes were tested for reverse osmosis. **Figure 9** and **Table 3** shows key performance parameters including flux and salt rejection of the membranes when tested with 25,000 ppm NaCl as feed. The flux through all membranes with CNS is higher than that of PVA-NC. However, the focus of this work is to study the effect of adding conductive carbon nanostructures to previously fabricated PVA-NC membranes in order to demonstrate electrolytic cleaning. As indicated in **Figure 9**, the flux is greatest for the membrane with the largest filler content. The polymer chains tend to form compressed packing structures when subjected to high pressures. This tendency to compress is disrupted by the presence of nano-fillers such as carbon nanostructures, and lower compression causes greater water flux through the membrane [19, 20]. Although the membranes demonstrate high salt rejection rates (above 99.7%), and the flux in the modified membranes is greater than that in PVA-NC alone, flux values are still low compared to commercial thin film composite (TFC) RO membranes. This is due to two main factors. First, the thickness of these self-supporting membranes is between 175 and 218 μm, which contributes to mass transfer resistance across the membrane. Second, the driving force, i.e. the transmembrane pressure, was kept at 24 bars, which is significantly less than typical pressures of 60-80 bars applied for seawater RO. According to the van't Hoff equation, the osmotic pressure for a feed solution with TDS 25,000 ppm is 19.4 bars. In RO, the driving force is the difference in applied pressure and osmotic pressure. In the RO experiments carried out in this work, the applied pressure is 24 bars which results in a transmembrane pressure of only 4.6 bars. The applied pressure should thus be increased to

obtain higher flux through the membrane for the treatment of given feed salinity. Although the freeze-drying step to open up the membrane structure was eliminated, the flux obtained is still comparable to freeze dried PVA-NC membranes in a previous study [13]. This is because pure water was first permeated through the membrane to open up the structure and enable water permeation during RO, without the additional step of freeze drying during membrane fabrication.

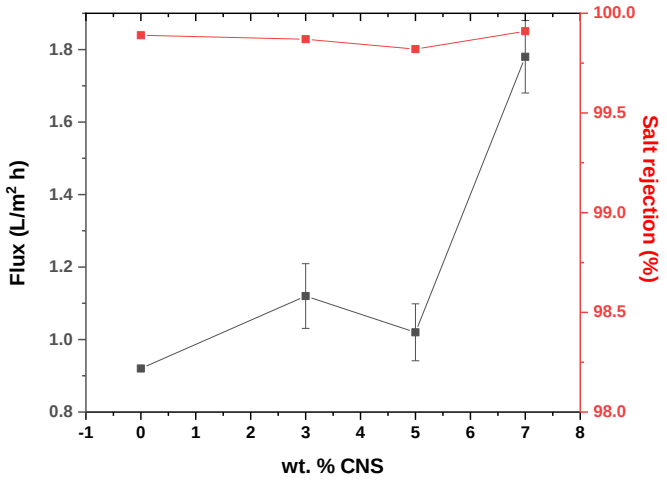

Figure 9: Flux and salt rejection for PVA-NC-CNS membranes with varying CNS content; RO test carried out at pressure of 24 bars with 25,000 ppm NaCl

Table 1: RO performance data for PVA-NC-CNS membranes

	Thickness (µm)	**Pure water flux J_0 (L/m² h)**	**Flux J (L/m² h)**	**Salt rejection (%)**
PVA-NC-0CNS	218 ± 4	0.815	0.92	99.89
PVA-NC-3CNS	179 ± 20	1.43	1.12	99.87
PVA-NC-5CNS	175 ± 21	1.22	1.02	99.82
PVA-NC-7CNS	203 ± 18	1.935	1.78	99.91

3.7 Electrolysis

Seawater RO membranes are prone to fouling by natural organic matter (NOM), such as humic acid (HA) [21]. To verify the effectiveness of conductive PVA-NC-CNS membranes for foulant removal via electrolysis, the membranes were first fouled by HA. Electrolysis was carried out on the fouled PVA-NC-7CNS membrane for 20 minutes, by applying a potential of -5 V, using 35000 PPM NaCl in DI water as electrolyte and a Pt rod counter-electrode. A relatively stable current of 7.5 mA was present during electrolytic cleaning, which according to the membrane area using during electrolysis is equivalent to 3.75 mA/cm^2. The resulting current was recorded as a function of time, and is shown in Figure 10. Optical images of the membrane before and after electrolysis (Figure 11) indicate that electrolysis was effective in removal of foulant from the membrane surface. The foulant is clearly visible before electrolysis (Figure 11a), while the membrane observed after electrolysis shows a clean surface (Figure 11b). Similarly, the foulant released from the membrane surface into the electrolyte is evident in photographs of the electrolyte taken before and after electrolytic cleaning (Figure 11 c and d). CNS was incorporated to improve the performance of PVA-NC membranes and render them conductive, allowing electrolytic cleaning for removal of foulants.

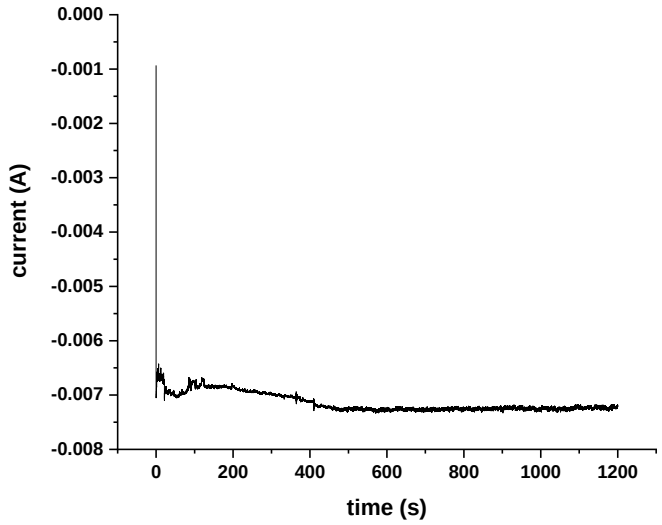

Figure 10: Current-time behavior during electrolysis with an applied voltage of -5V on the membrane

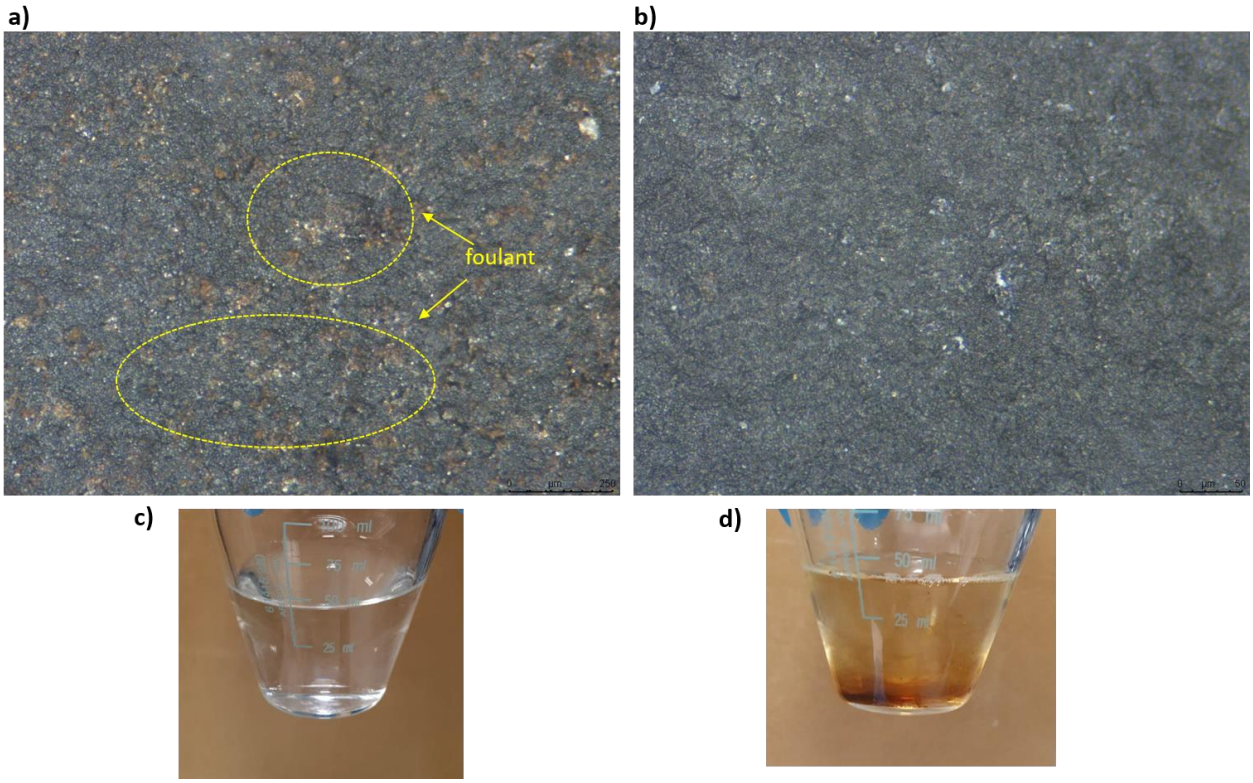

Figure 11: Digital images of a) fouled PVA-NC-7CNS membrane before electrolysis and b) fouled PVA-NC-7CNS membrane after electrolysis at -5V for 20 minutes; c) and d) show photographs of the electrolyte before and after electrolytic cleaning of membrane

4. Conclusion

In this work, PVA membranes were modified using a conductive form of networked cellulose, made by incorporating carbon nanostructures in NC, also known as NC-CNS. Using NC-CNS improved the mechanical strength of the membranes as compared to NC alone, and increased the RO flux by 93%. The enhanced membranes demonstrated enhanced electrocatalytic activity for hydrogen evolution in acidic medium, which can further be used for in situ membrane cleaning via electrochemical methods. The efficiency of the membranes for electrolytic cleaning was demonstrated using humic acid and yeast as foulants. Future work includes investigating the effect of adding a conductive layer to the membrane-electrolyte surface as opposed to modifying the bulk material and incorporating these novel membranes for electrically enhanced RO.

6. References

1. WWAP, The United Nations World Water Development Report 2018: Nature-based Solutions. 2018, UNESCO: Paris.

2. Research, O., Global Water Desalination Market: 2018-2025 Key Industry Insights, Segments, Opportunities, and Forecasts. 2018.

3. Qasim, M., et al., Reverse osmosis desalination: A state-of-the-art review. Desalination, 2019. **459**: p. 59-104.

4. Choi, H.-g., M. Son, and H. Choi, Integrating seawater desalination and wastewater reclamation forward osmosis process using thin-film composite mixed matrix membrane with functionalized carbon nanotube blended polyethersulfone support layer. Chemosphere, 2017. **185**: p. 1181-1188.

5. Cheng, X., et al., Improving ultrafiltration membrane performance with pre-

deposited carbon nanotubes/nanofibers layers for drinking water treatment. Chemosphere, 2019. **234**: p. 545-557.

6. Rahaman, M.S., C.D. Vecitis, and M. Elimelech, Electrochemical carbon-nanotube filter performance toward virus removal and inactivation in the presence of natural organic matter. Environmental science & technology, 2012. **46**(3): p. 1556-1564.

7. Wang, S., et al., In-situ combined dual-layer CNT/PVDF membrane for electrically-enhanced fouling resistance. Journal of Membrane Science, 2015. **491**: p. 37-44.

8. Ahmed, F., et al., Electrically conductive polymeric membranes for fouling prevention and detection: A review. Desalination, 2016. **391**: p. 1-15.

9. Dudchenko, A.V., et al., Organic fouling inhibition on electrically conducting carbon nanotube–polyvinyl alcohol composite ultrafiltration membranes. Journal of membrane science, 2014. **468**: p. 1-10.

10. Ahmed, F.E., et al., Electrically conducting nanofiltration membranes based on networked cellulose and carbon nanostructures. Desalination, 2017. **406**: p. 60-66.

11. Duan, W., et al., Electrochemical mineral scale prevention and removal on electrically conducting carbon nanotube–polyamide reverse osmosis membranes. Environmental Science: Processes & Impacts, 2014. **16**(6): p. 1300-1308.

12. Liu, Q., et al., An effective design of electrically conducting thin-film composite (TFC) membranes for bio and organic fouling control in forward osmosis (FO). Environmental Science & Technology, 2016. **50** (19): p. 10596-10605.

13. Anis, S.F., B.S. Lalia, and R. Hashaikeh, Controlling swelling behavior of poly (vinyl) alcohol via networked cellulose and its application as a reverse osmosis membrane.

Desalination, 2014. **336**: p. 138-145.

14. Hashaikeh, R. and H. Abushammala, Acid mediated networked cellulose: Preparation and characterization. Carbohydrate Polymers, 2011. **83**(3): p. 1088-1094.

15. Wu, J., et al., Improving the hydrophilicity and fouling resistance of RO membranes by surface immobilization of PVP based on a metal-polyphenol precursor layer. Journal of Membrane Science, 2015. **496**: p. 58-69.

16. Lee, S., W.S. Ang, and M. Elimelech, Fouling of reverse osmosis membranes by hydrophilic organic matter: implications for water reuse. Desalination, 2006. **187**(1): p. 313-321.

17. Bin, Y., et al., Morphology and mechanical and electrical properties of oriented PVA–VGCF and PVA–MWNT composites. Polymer, 2006. **47**(4): p. 1308-1317.

18. Probst, O., et al., Nucleation of polyvinyl alcohol crystallization by single-walled carbon nanotubes. Polymer, 2004. **45**(13): p. 4437-4443.

19. Kim, H.J., et al., High-Performance Reverse Osmosis CNT/Polyamide Nanocomposite Membrane by Controlled Interfacial Interactions. ACS Applied Materials & Interfaces, 2014. **6**(4): p. 2819-2829.

20. Kong, C., et al., Controlled synthesis of high performance polyamide membrane with thin dense layer for water desalination. Journal of Membrane Science, 2010. **362**(1): p. 76-80.

21. Zhu, R., et al., Mechanism of humic acid fouling in a photocatalytic membrane system. Journal of Membrane Science, 2018. **563**: p. 531-540.